

Supporting Information

For

Solution properties of the Ln^{III} complexes of a novel octadentate chelator with rigidified iminodiacetate arms

Lorenzo Tei^[a], Zsolt Baranyai^[b], Claudio Cassino^[a], Marianna Fekete^[a], Ferenc K. Kálmán^[b] and
Mauro Botta*^[a]

^a Dipartimento di Scienze ed Innovazione Tecnologica, Università del Piemonte Orientale “Amedeo Avogadro” Viale T. Michel 11, I-15121, Alessandria, Italy;

^b Department of Inorganic and Analytical Chemistry, University of Debrecen,
H-4010, Debrecen, Egyetem tér 1., Hungary

Contents:

1. Protonation and complexation equilibria (p. 2)
2. Kinetic studies (p. 4)
3. Variable temperature ¹H and ¹³C NMR spectra (p. 9)
4. Relaxometric properties (p. 14)

1. Protonation and complexation equilibria

The protonation constants of the ligand are defined by Equation (1):

$$K_i^H = \frac{[H_iL]}{[H_{i-1}L][H^+]} \quad (1)$$

where $i=1, 2 \dots 4$. These were determined by both pH-potentiometric and $^1\text{H-NMR}$ titrations. At different pH values, $^1\text{H NMR}$ signals display sharp changes related to the protonation of the ligand. Since the protonation/deprotonation of the different donor atoms is generally fast process on the NMR time scale, the chemical shifts of the observed signals represent a weighted average of the shifts of the different species involved in a specific protonation step (Eq. 2):

$$\delta_{H(\text{obs})} = \sum x_i \delta_H^{H_iL} \quad (2)$$

where, $\delta_{H(\text{obs})}$ is the observed chemical shift of a given signal, x_i and $\delta_H^{H_iL}$ are the molar fraction and the chemical shift of the involved species, respectively (the molar fractions x_i of the different protonated species are expressed with the use of the protonation constants K_i^H).

The stability and protonation constants of the metal complexes formed with the chelating ligands **L1** and EGTA are defined by Equations (3) and (4). The best fitting was obtained by using the model which includes the formation of *ML* and *MHL* species.

$$K_{\text{ML}} = \frac{[\text{ML}]}{[\text{M}][\text{L}]} \quad (3)$$

$$K_{\text{MH}_i\text{L}} = \frac{[\text{MH}_i\text{L}]}{[\text{MH}_{i-1}\text{L}][\text{H}^+]} \quad (4)$$

where $i=1$. The titration data for **L1** and EGTA in the presence of Zn^{2+} and Cu^{2+} indicate base consuming process at $\text{pH}>9$. This process can be interpreted by assuming the coordination of OH^- ion according to Equation (5):

$$K_{\text{MLH}_{-1}} = \frac{[\text{ML}]}{[\text{M}(\text{OH})\text{L}][\text{H}^+]} \quad (5)$$

pH-potentiometric titrations were also made at 2:1 metal-to-ligand ratio in order to examine the possible formation of dinuclear Zn^{2+} and Cu^{2+} complexes. The stability and protonation constants of the dinuclear-, dinuclear-monohydroxo- and dinuclear-dihydroxo-complexes are defined by Equations (6), (7) and (8), respectively.

$$K_{M_2L} = \frac{[M_2L]}{[ML][M]} \quad (6)$$

$$K_{M_2LH_1} = \frac{[M_2L]}{[M_2(OH)L][H^+]} \quad (7)$$

$$K_{M_2LH_2} = \frac{[M_2(OH)L]}{[M_2(OH)_2L][H^+]} \quad (8)$$

As explained in the text, in the presence and absence of Mg^{2+} ion the shape of the titration curve of **L1** is the same (Figure S1). The fitting of the data obtained in these titrations did not give any reasonable result for the stability constant of the Mg^{2+} complex.

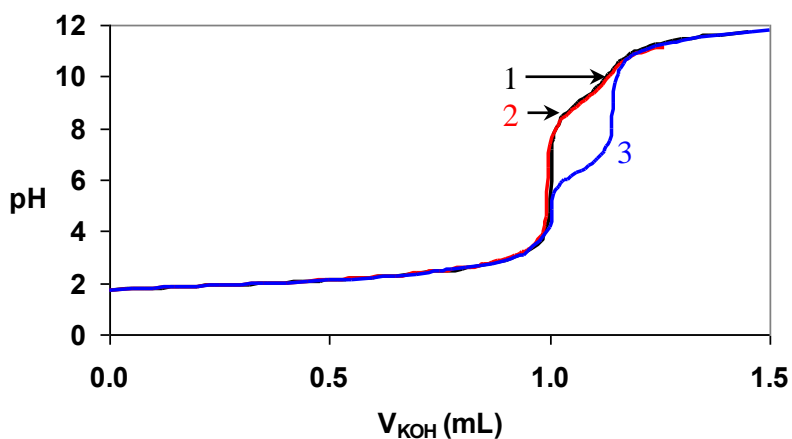


Figure S1. Titration curve of the H_4L1 ligand in the absence (1) and in the presence of Mg^{2+} (2) and Ca^{2+} (3) ($[H_4L1]=[Mg^{2+}]=[Ca^{2+}]=2$ mM, $[HCl]=16$ mM, $[KOH]=0.2$ M, 0.1 M KCl, 25°C)

2. Kinetic studies

The rates of the transmetallation reactions of $[\text{Gd}(\text{L1})]^-$ and $[\text{Gd}(\text{EGTA})]^-$ were studied by UV-spectrophotometry with the use of Cu^{2+} and Eu^{3+} as exchanging metal ions. In the presence of excess of the exchanging ion the transmetallation can be treated as a pseudo-first-order process and the reaction rate can be expressed with the Eq. (9), where k_d is a pseudo-first-order rate constant, $[\text{GdL}]_t$ and $[\text{GdL}]_{\text{tot}}$ are the concentrations of the GdL species at time t and the total concentration of the complex, respectively.

$$-\frac{d[\text{GdL}]_t}{dt} = k_d[\text{GdL}]_{\text{tot}} \quad (9)$$

The rates of the transmetallation reactions were studied at different concentrations of the exchanging ions in the pH range 4.0 – 6.3. The obtained rate constants k_d are presented as a function of the pH in Figures S2, S3, S4 and S5.

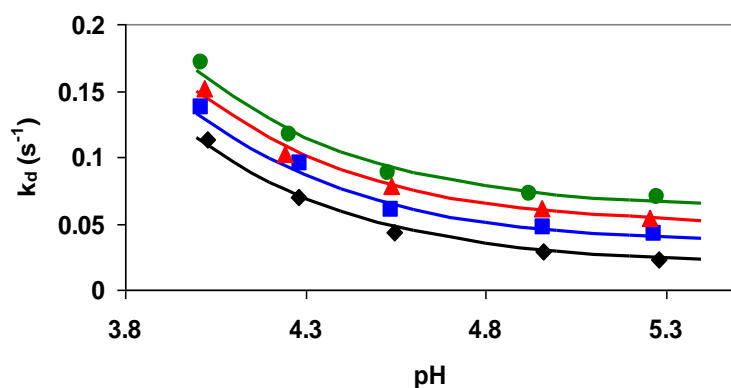


Figure S2. Pseudo-first order rate constants (k_d) of the metal exchange reactions of $[\text{GdL1}]^-$ with Cu^{2+} ions as a function of pH ($[\text{Gd}(\text{L1})]^- = 0.1 \text{ mM}$, $[\text{Cu}^{2+}] = 1 \text{ mM}$ (◆), 2 mM (■), 3 mM (▲) and 4 mM (●); 0.1 M KCl , $25 \text{ }^\circ\text{C}$)

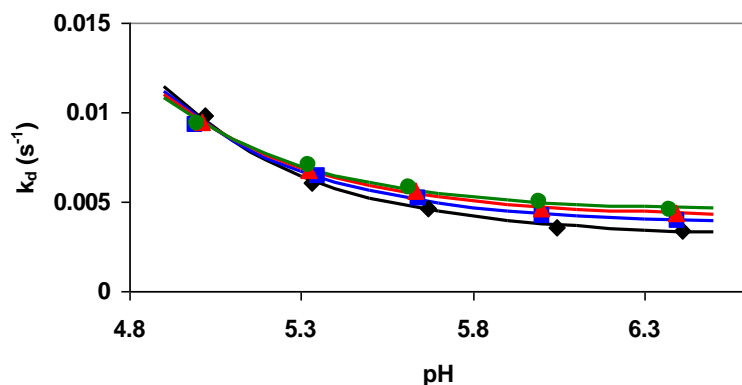


Figure S3. Pseudo-first order rate constants (k_d) of the metal exchange reactions of $[\text{Gd(L1)}]^-$ with Eu^{3+} ions as a function of pH ($[\text{Gd(L1)}]^- = 0.5 \text{ mM}$, $[\text{Eu}^{3+}] = 10 \text{ mM}$ (◆), 15 mM (■), 20 mM (▲) and 25 mM (●); 0.1 M KCl , $25 \text{ }^\circ\text{C}$)

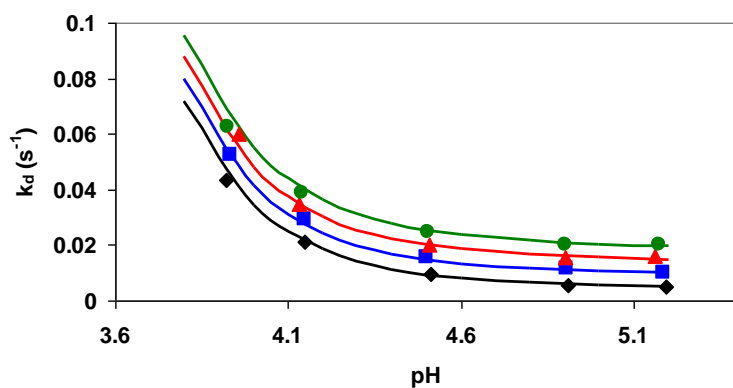


Figure S4. Pseudo-first order rate constants (k_d) of the metal exchange reactions of $[\text{Gd(EGTA)}]^-$ with Cu^{2+} ions as a function of pH ($[\text{Gd(EGTA)}]^- = 0.1 \text{ mM}$, $[\text{Cu}^{2+}] = 1 \text{ mM}$ (◆), 2 mM (■), 3 mM (▲) and 4 mM (●); 0.1 M KCl , $25 \text{ }^\circ\text{C}$)

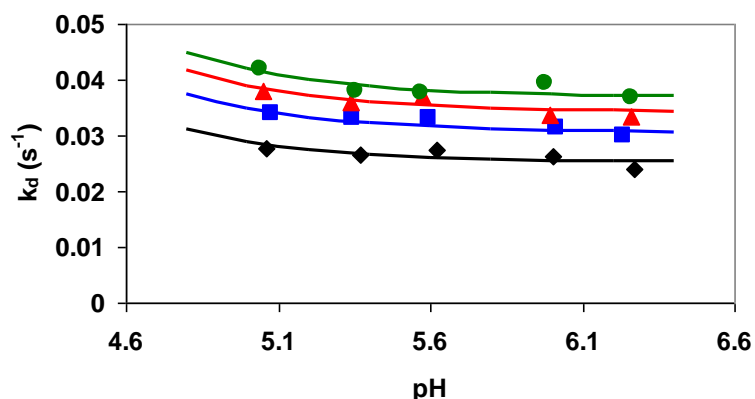
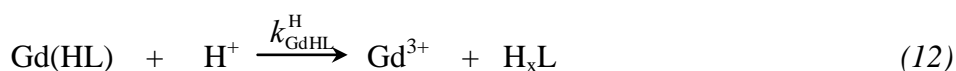
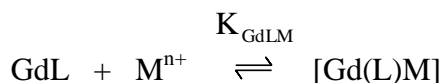


Figure S5. Pseudo-first order rate constants (k_d) of the metal exchange reactions of $[\text{Gd}(\text{EGTA})]^-$ with Eu^{3+} ions as a function of pH ($[\text{Gd}(\text{EGTA})]^- = 1.0 \text{ mM}$, $[\text{Eu}^{3+}] = 20 \text{ mM}$ (♦), 30 mM (■), 40 mM (▲) and 50 mM (●); 0.1 M KCl , $25 \text{ }^\circ\text{C}$).

These figures show that k_d values exhibit a similar dependence in the reactions with Cu^{2+} and Eu^{3+} . k_d values increase with increase of $[\text{H}^+]$ and also with increasing $[\text{Cu}^{2+}]$ or $[\text{Eu}^{3+}]$ at $\text{pH} > 4.5$. The increase in k_d values with increasing H^+ concentration can be interpreted in terms of proton assisted dissociation of $[\text{Gd}(\text{L1})]^-$ and $[\text{Gd}(\text{EGTA})]^-$ followed by a fast reaction between free ligand and exchanging metal ions (Cu^{2+} or Eu^{3+}). The dependence of k_d on $[\text{H}^+]$ can be expressed as a first- and second-order function of $[\text{H}^+]$ which indicates that the exchange can take place by proton-independent (Eq. 10) and proton assisted (Eqs. 11 and 12) pathways. The proton assisted dissociation of $[\text{Gd}(\text{L1})]^-$ and $[\text{Gd}(\text{EGTA})]^-$ can be explained by the formation of a protonated $[\text{Gd}(\text{HL1})]$ and $[\text{Gd}(\text{HEGTA})]$ complexes, which dissociate through spontaneous (Eq. 11) and proton-assisted (Eq. 12) pathways.



The increase in exchange reaction rate with increasing $[\text{Cu}^{2+}]$ or $[\text{Eu}^{3+}]$ indicates that the reaction can take place by direct attack of the exchanging metal ion to the complex, via formation of dinuclear intermediates (Eq. 13).

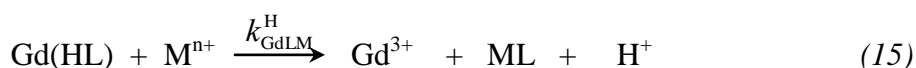


$$K_{\text{GdLM}} = \frac{[\text{Gd(L)M}]}{[\text{Gd(L)}][\text{M}^{n+}]} \quad (13)$$

It can be assumed that in the dinuclear intermediate $[\text{Gd(L)M}]$, the functional groups of **L1** and EGTA are slowly transferred from the Gd^{3+} to the attacking Cu^{2+} or Eu^{3+} step by step (Eq. 14).



At $\text{pH} < 4.5$, the exchanging metal ions attack the protonated $[\text{Gd(HL1)}]$ and $[\text{Gd(HEGTA)}]$. In case of protonated and dinuclear complexes, the functional groups of **L1** and EGTA are weakly coordinated to the Gd^{3+} ion and they slowly transfer from the Gd^{3+} to the attacking Cu^{2+} and Eu^{3+} ions (Eq. 15).



The k_0 , k_{GdHL} , $k_{\text{GdHL}}^{\text{H}}$, k_{GdLM} and $k_{\text{GdLM}}^{\text{H}}$ rate constants characterize the dissociation of $[\text{Gd(L1)}]^-$ and $[\text{Gd(EGTA)}]^-$ via spontaneous, proton-assisted, metal-assisted and proton-metal-assisted (when the exchanging metal attacks the protonated complexes) reaction pathways, respectively. The K_{GdHL} and K_{GdLM} are the protonation constants of the protonated complexes and the stability constant of the mixed dinuclear intermediate complexes, respectively (where $K_{\text{GdHL}} = [\text{Gd(HL)}]/[\text{Gd(L)}][\text{H}^+]$, $K_{\text{GdLM}} = [\text{Gd(L)M}]/[\text{Gd(L)}][\text{M}]$). The protonation constant of the $[\text{Gd(L1)}]^-$ and $[\text{Gd(EGTA)}]^-$ complexes were determined by pH-potentiometric titration ($[\text{Gd(L1)}]^-$: $\log K_{\text{MHL}} = 3.07$; $[\text{Gd(EGTA)}]^-$: $\log K_{\text{MHL}} = 1.89$ in Table 2) and used for the calculation of the kinetic parameters.

By taking into account all the possible pathways and the rate of the transmetallation of $[\text{Gd(L1)}]^-$ and $[\text{Gd(EGTA)}]^-$ (Eq. 9), the pseudo-first-order rate constant (k_d) can be defined by Equation (16).

$$-\frac{[\text{GdL}]_t}{dt} = k_0[\text{GdL}] + k_{\text{GdHL}}[\text{Gd(HL)}] + k_{\text{GdHL}}^{\text{H}}[\text{Gd(HL)}][\text{H}^+] + k_{\text{GdLM}}[\text{Gd(L)M}] + k_{\text{GdLM}}^{\text{H}}[\text{Gd(HL)}][\text{M}] \quad (16)$$

By taking into account the total concentration of the complex ($[\text{GdL}]_{\text{tot}} = [\text{GdL}] + [\text{Gd(HL)}] + [\text{Gd(L)M}]$) and the equations of protonation and stability constants of the intermediates (K_{GdHL} and K_{GdLM}), the pseudo-first-order rate constant can be expressed as follows:

$$k_d = \frac{k_0 + k_1[\text{H}^+] + k_2[\text{H}^+]^2 + k_3[\text{M}^{\text{n}+}] + k_4[\text{M}][\text{H}^+]}{1 + K_{\text{GdHL}}[\text{H}^+] + K_{\text{GdLM}}[\text{M}]} \quad (17)$$

where, k_0 , and $k_1 = k_{\text{GdHL}} \cdot K_{\text{GdHL}}$, $k_2 = k_{\text{GdHL}}^{\text{H}} \cdot K_{\text{GdHL}}$, $k_3 = k_{\text{GdLM}} \cdot K_{\text{GdLM}}$ and $k_4 = k_{\text{GdLM}}^{\text{H}} \cdot K_{\text{GdHL}}$ characterize the spontaneous, proton-, metal- and proton-metal-assisted dissociation of $[\text{Gd(L1)}]^-$ and $[\text{Gd(EGTA)}]^-$, respectively. Rate constants, protonation and stability constants have been calculated by fitting the k_d values to the Eq. (17).

3. Variable temperature ^1H and ^{13}C NMR spectra

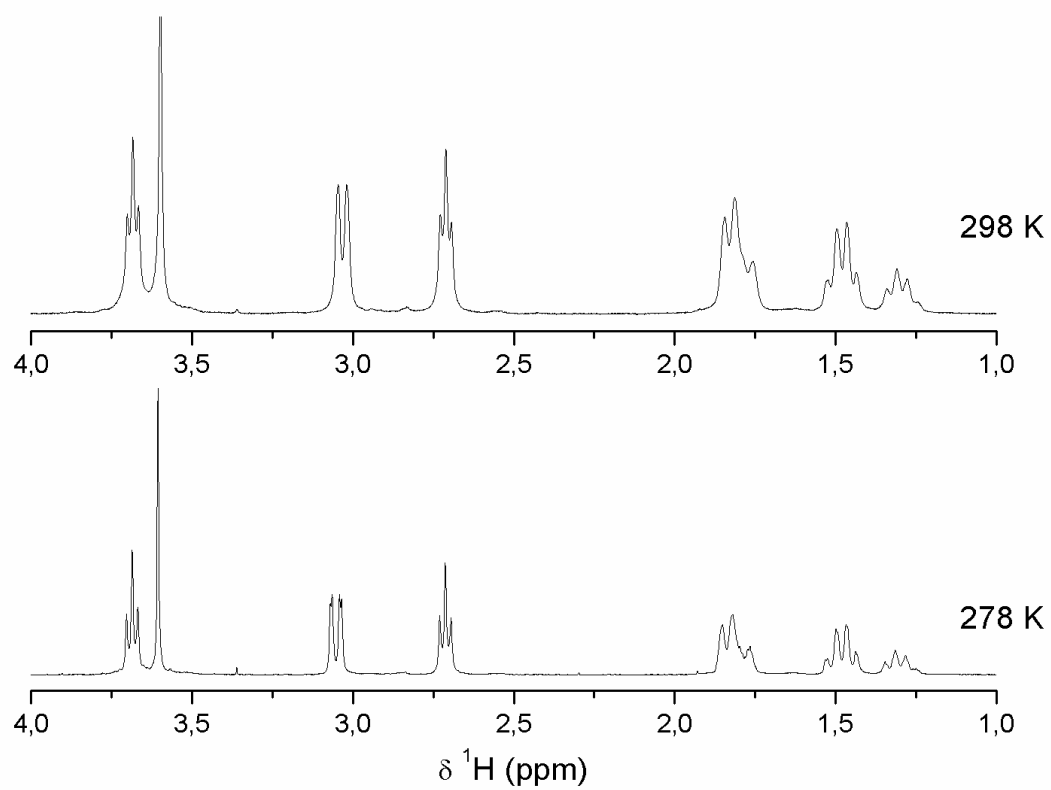


Figure S6. VT ^1H NMR spectra for $[\text{La}(\text{L1})]^-$ at 9.4 T.

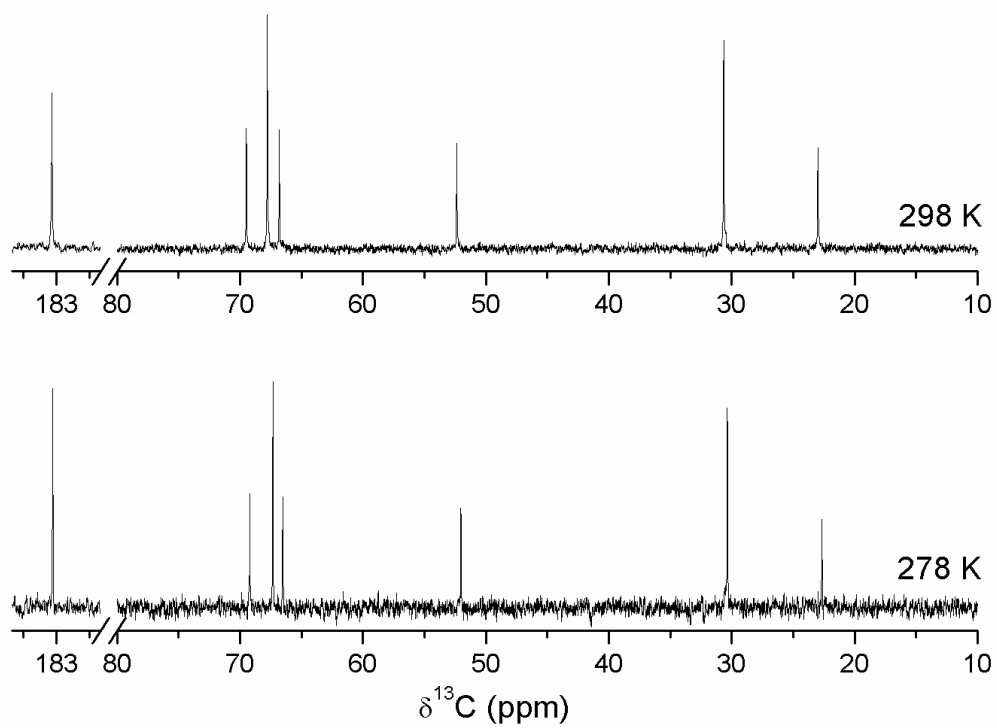


Figure S7. VT ^{13}C NMR spectra for $[\text{La}(\text{L1})]^-$ at 9.4 T.

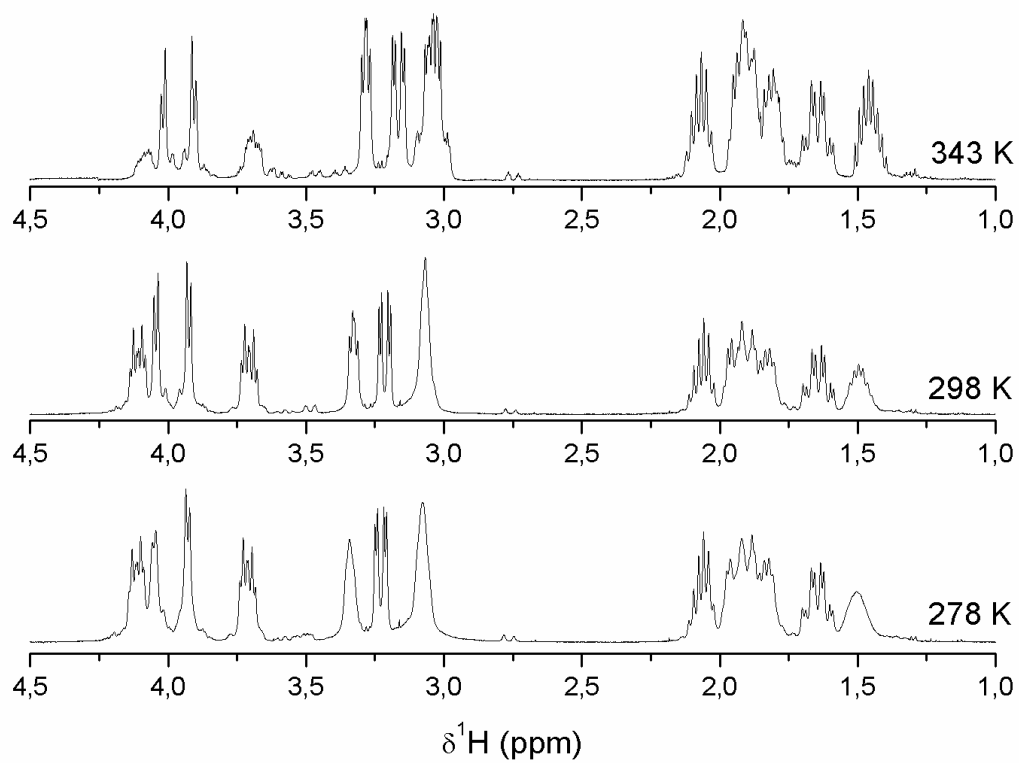


Figure S8. VT ^1H NMR spectra for $[\text{Lu}(\text{L1})]^-$ at 9.4 T.

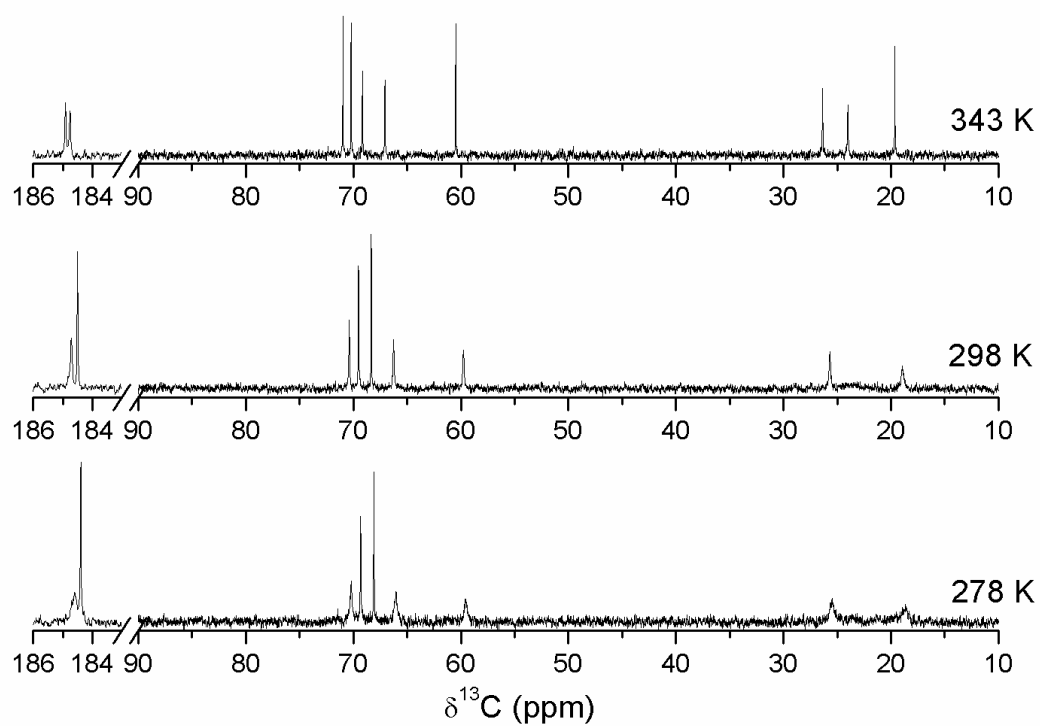


Figure S9. VT ^{13}C NMR spectra for $[\text{Lu}(\text{L1})]^-$ at 9.4 T.

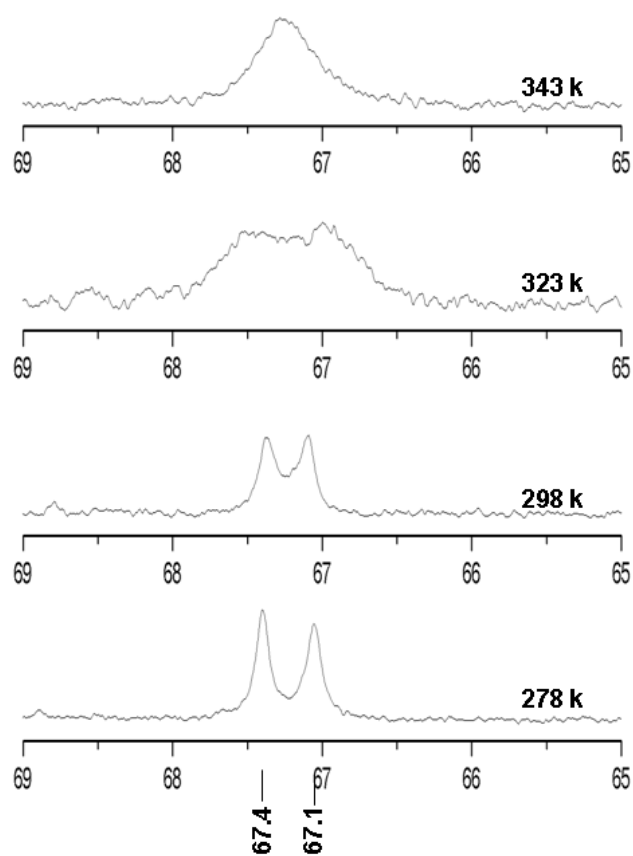


Figure S10. VT ^{13}C NMR spectra for $[\text{Y}(\text{L1})]^-$ at 9.4 T; magnification of the region of the $-\text{CH}$ carbons.

4. Relaxometric properties

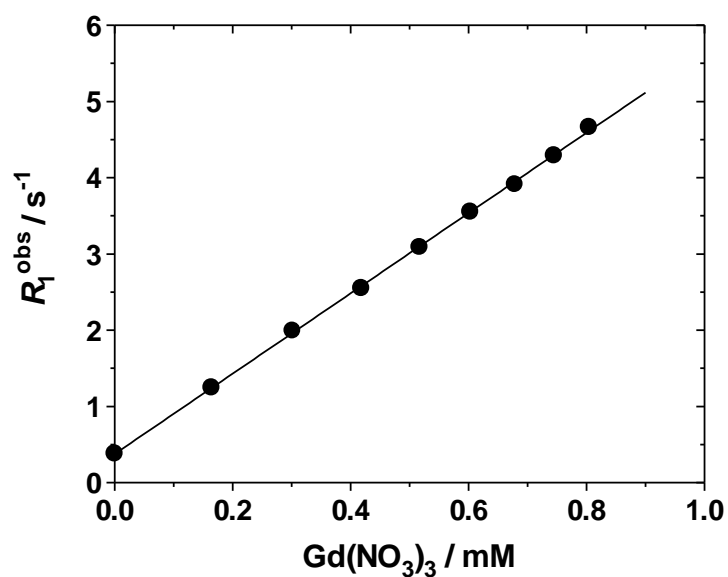


Figure S11. Variation of the relaxation rate, at 20 MHz and 298 K, of a 0.8 mM solution of **L1** following stepwise additions of a stock solution of Gd(NO₃)₃. A large and non linear increase of R_1 indicates that the Gd/**L1** ratio is higher than one. In that case a further small addition of ligand restores the 1:1 molar ratio and the R_1 value returns to the straight line. The slope of the line ($5.2 \text{ mM}^{-1} \text{ s}^{-1}$; $R=0.9998$) corresponds to the r_{1p} value of $[\text{Gd}(\text{L1})]^-$.

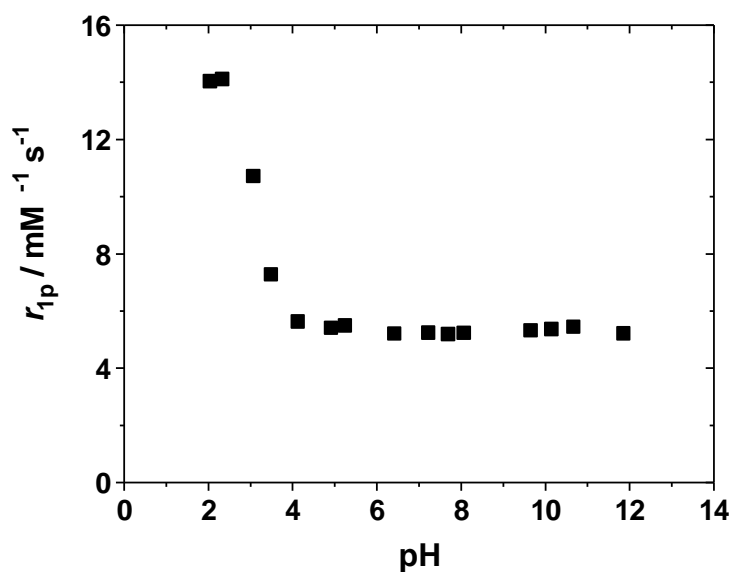


Figure S12. Plot of R_1 of $[\text{Gd}(\text{L1})]^-$ on pH variation (20 MHz, 298 K).